Available online at www.sciencedirect.com

ScienceDirect

Geochimica et Cosmochimica Acta 300 (2021) 231–245

Geochimica et Cosmochimica Acta

www.elsevier.com/locate/gca

Spectrophotometric determination of the bicarbonate dissociation constant in seawater

Katelyn M. Schockman, Robert H. Byrne *

College of Marine Science, University of South Florida, 140 7th Avenue South, St. Petersburg, FL 33701, USA

Received 28 March 2020; accepted in revised form 5 February 2021; available online 15 February 2021

Abstract

The aqueous carbon dioxide (CO_2) system stoichiometric dissociation constants K_1 and K_2 express the relative concentrations of CO_2, HCO_3^- (bicarbonate), and CO_3^{2-} (carbonate) in terms of pH. These constants are critical in the study of seawater and the oceans because any mathematical expression that relates the four major CO_2 system parameters (pH, here expressed on the total hydrogen ion concentration scale, pH_T; total dissolved inorganic carbon, C_T; total alkalinity, A_T; and CO_2 fugacity, fCO_2) requires the use of K_1 and K_2. Uncertainties associated with current characterizations of pK_1 and pK_2 (where $pK = -\log K$), on the order of 0.01 and 0.02, limit the accuracy of marine CO_2 system calculations. This work reports the results of a spectrophotometric method to experimentally determine the product K_1K_2 over environmentally relevant ranges of temperature ($288.15 \leq T \leq 308.15$ K) and salinity ($19.6 \leq S_p \leq 41$) where S_p denotes the practical salinity scale. Using previously published parameterizations of K_1, values of pK_2 could then be calculated from the new K_1K_2 values. The resulting set of pK_2 values was fitted as a function of S_p and T to obtain a new pK_2 parameterization (denoted as ${}_{SW}pK_2$) calculated with the K_1 of Waters and Millero (2013) as revised by Waters et al. (2014): ${}_{SW}pK_2 = 116.8067 - 3655.02\ T^{-1} - 16.45817\ \ln T + 0.04523\ S_p - 0.615\ S_p^{0.5} - 0.0002799\ S_p^2 + 4.969\ (S_p/T)$

The average root mean square deviation between the equation and the observed data is 0.003. Residuals of this pK_2 fitting function (i.e., measured pK_2 minus parameterized pK_2) are substantially smaller than the residuals obtained in previous works. Similarly, the total standard uncertainty in pK_2 is reduced from 0.015 (previous characterizations) to 0.010 (this work). Internal consistency assessments (comparisons of measured versus calculated values of A_T, C_T, pH_T, and fCO_2) were used to evaluate the computational utility of the new K_2 parameterization. Assessments from both laboratory and shipboard data indicate that the internal consistency of CO_2 system calculations is improved using the K_2 parameterization of this work. This new K_2 parameterization provides the most precise, and potentially the most accurate, bicarbonate dissociation constant characterization presently available for open ocean conditions.

Keywords: CO_2 system; Dissociation constant; Internal consistency; Seawater; Carbonate

1. INTRODUCTION

Throughout the industrial era (1750s–present), approximately 30% of anthropogenic carbon dioxide (CO_2) emissions has been absorbed by the world's oceans (Le Quéré et al., 2018; Gruber et al., 2019). The resulting increase of CO_2 in ocean seawater has changed its chemical composition by decreasing pH by approximately 0.1 over this time period and lowering carbonate ion concentration (Caldeira and Wickett, 2003; Bates et al., 2014; Byrne, 2014). Consistent with this extent of ocean acidification, decreases in the calcium carbonate ($CaCO_3$) saturation states of seawater

* Corresponding author.
E-mail addresses: kschockman@usf.edu (K.M. Schockman), rhbyrne@usf.edu (R.H. Byrne).

https://doi.org/10.1016/j.gca.2021.02.008
0016-7037/

($\Omega_{calcite}$ and $\Omega_{aragonite}$) have begun to negatively affect calcifying organisms (Riebesell et al., 2000; Feely et al., 2004; Doney et al., 2012; Wittmann and Pörtner, 2013). Changes in the CO_2 system have also led to regional variations in the buffer capacity of seawater (Carter et al., 2017; Woosley, 2018). Additionally, increased warming and changing ocean circulation have caused fluctuations in the oceanic uptake of atmospheric CO_2 over time, with the magnitude of CO_2 fluxes in or out of the ocean varying not only through time but also by oceanic region (Gruber et al., 2019).

The CO_2 system in seawater includes dissolved carbon dioxide (CO_2^*=$CO_{2(aq)} + H_2CO_3$), bicarbonate (HCO_3^-), and carbonate (CO_3^{2-}). Constituent equilibria that involve the exchange of H^+ ions are:

$$CO_2^* + H_2O \leftrightarrow HCO_3^- + H^+ \quad (1)$$

$$HCO_3^- \leftrightarrow CO_3^{2-} + H^+ \quad (2)$$

These equilibria constitute the ocean's principal pH buffering mechanism.

The seawater CO_2 system can be described using four measurable parameters: total alkalinity (A_T), total dissolved inorganic carbon (C_T), pH, and CO_2 fugacity (fCO_2). The first three are defined as follows:

$$A_T = [HCO_3^-]_T + 2[CO_3^{2-}]_T + [B(OH)_4^-]_T + [OH^-]_T - [H^+]_T + 2[PO_4^{3-}]_T + [HPO_4^{2-}]_T + \ldots \quad (3)$$

$$C_T = [CO_3^{2-}]_T + [HCO_3^-]_T + [CO_2^*] \quad (4)$$

$$pH_T = -\log [H^+]_T \quad (5)$$

The subscripted brackets ($[\ ]_T$) generally denote free plus ion-paired concentrations (where concentration is measured in mol kg-soln^{-1}), whereas $[H^+]_T$ denotes the sum of free hydrogen and bisulfate ions, pH_T denotes pH on the total hydrogen ion concentration scale, and the ellipses in Eq. (3) and throughout indicate additional terms of generally smaller quantitative importance. For Eq. (3), these excluded species may add uncertainty in the accuracy of calculated carbonate alkalinity.

Measurement of any two of the four parameters allows for calculation of all other CO_2 system parameters via thermodynamic relationships. Essentially all descriptions of CO_2 system parameters at in-situ conditions require thermodynamic models. For example, pH_T at in-situ conditions can be calculated through an iterative approach from C_T and A_T:

$$A_T = C_T\left(\frac{2K_1K_2 + K_1[H^+]_T}{K_1K_2 + K_1[H^+]_T + [H^+]_T^2}\right) + B_T\left(\frac{K_B}{K_B + [H^+]_T}\right) + K_w[H^+]_T^{-1} - [H^+]_T + \ldots \quad (6)$$

where additional terms of minor importance are omitted for simplicity. B_T is the total boron concentration, K_B and K_W are equilibrium constants that describe the dissociation of boric acid and water, and K_1 and K_2 are stoichiometric equilibrium constants appropriate to the equilibria shown in Eqs. (1) and (2), defined as follows:

$$K_1 = \frac{[HCO_3^-]_T[H^+]_T}{[CO_2^*]} \quad (7)$$

$$K_2 = \frac{[CO_3^{2-}]_T[H^+]_T}{[HCO_3^-]_T} \quad (8)$$

where $[H^+]_T$ is expressed on the total hydrogen ion concentration scale. The use of Eq. (6) to accurately derive in-situ $[CO_3^{2-}]_T$ and other CO_2 system parameters (e.g., $\Omega_{calcite}$, $\Omega_{aragonite}$, fCO_2, or pH_T) requires an accurate account of the dependencies of relevant dissociation constants (K_1, K_2, K_B, and K_W) on salinity (S), temperature (t in °C or T in K), and pressure (P) (Fong and Dickson, 2019).

Over-determination of the system (i.e., where three or more CO_2 system parameters are measured for a single seawater sample) allows for comparisons of measured and calculated values of the same parameter and, as such, evaluations of its internal consistency. Current models that relate A_T, C_T, pH_T, and fCO_2 are not internally consistent (e.g., A_T (measured) ≠ A_T (calculated) from C_T and pH_T) (Patsavas et al., 2015; Fong and Dickson, 2019). Furthermore, the differences between calculated and measured parameters are larger than what would be expected based on previously reported measurement accuracies and precisions (Mojica Prieto and Millero, 2002; Millero et al., 2006). Accurate characterizations of the dissociation constants K_1 and K_2 are arguably the most critically important elements for obtaining internal consistency and, thereby, accurate predictions of in-situ parameters.

Throughout the past several decades, extensive effort has been devoted to experimentally determine stoichiometric carbonic acid dissociation constants over ranges of S and T (Hansson, 1973; Mehrbach et al., 1973; Goyet and Poisson, 1989; Roy et al., 1993; Millero et al., 2002, 2006; Mojica Prieto and Millero, 2002; Papadimitriou et al., 2018). Still, the K_1 and K_2 parameterizations obtained in these studies produced calculated values of CO_2 system parameters that do not agree within the estimated parameter uncertainties (Dickson and Millero, 1987; Lee et al., 2000). Uncertainties for pK_1 and pK_2 (where $pK = -\log K$) have been recently estimated as 0.0075 and 0.015, respectively (Orr et al., 2018). Based on internal consistency checks, several publications have concluded that the K_1 and K_2 values of Mehrbach et al. (1973), as refit by Dickson and Millero (1987) on the seawater pH scale (SWS) and refit by Lueker et al. (2000) on the total hydrogen ion concentration pH scale (pH_T), provide the most internally consistent characterizations to date (Lee et al., 1996, 2000; Wanninkhof et al., 1999; Lueker et al., 2000; Patsavas et al., 2015). Notably, however, the study of Sulpis et al. (2020) found that the parameterizations of Lueker et al. (2000) overestimate K_1 and K_2 at low temperatures, and an overall lack of agreement between sets of constants led Naviaux et al. (2019) to recommend that new values of K_1 and K_2 be evaluated. Waters and Millero (2013), as revised by Waters et al. (2014), used a Pitzer model to refit data from Mehrbach et al. (1973), Mojica Prieto and Millero (2002), and Millero et al. (2006) to provide an updated set of K_1 and K_2 parameterizations, but a thorough assessment of internal consistency with these parameterizations has not been carried out.

Most previous characterizations of K_1 and K_2 have relied on acid titrations and, consequently, are dependent

on accurate assessments of several additional chemical parameters. These parameters include the boron/salinity ratio (B_T/S) (which currently has a relative uncertainty on the order of 2–3% (Orr et al., 2018; Fong and Dickson, 2019)), as well as K_B, K_W, and the concentrations and dissociation characteristics of all minor acid/base pairs in solution. Experimental determinations of the product K_1K_2, used by Mehrbach et al. (1973) and Mojica Prieto and Millero (2002), do not require acid titrations and furthermore are largely independent of several chemical parameter characteristics (B_T/S, K_B, K_W, minor acid/base pairs). This method is dependent on measured pH (as described below in Section 4) and, notably, has previously involved the use of either potentiometric methods or spectrophotometric measurements with unpurified pH indicators (Mehrbach et al., 1973; Mojica Prieto and Millero, 2002) — methods that can now be improved upon. Spectrophotometric pH measurements have a precision of approximately ±0.001 pH units or better (Yao and Byrne, 2001) and do not require periodic calibrations. The enhanced simplicity of spectrophotometric methods, compared to potentiometric methods, removes many systematic errors and is thereby conducive to improved accuracy.

In the present work, spectrophotometric procedures for measuring pH_T with a purified pH indicator are used to experimentally determine K_2 following the general procedures of Mehrbach et al. (1973). Use of the same procedures for measuring pH_T in field studies and for characterizing pK_2 (as in this work) enables improved CO_2 system assessments throughout the world's oceanic, estuarine, and riverine environments.

2. THEORY

The fundamental CO_2 system relationship that expresses A_T in terms of C_T and $[H^+]_T$ is shown in Eq. (6). Addition of a carbonate/bicarbonate salt to a mixture of seawater and added indicator dye at constant pH without diluting the solution is then appropriately described by:

$$A_T + A_T' = (C_T + C_T')\left(\frac{2K_1K_2 + K_1[H^+]_T}{K_1K_2 + K_1[H^+]_T + [H^+]_T^2}\right) + \Psi \quad (9)$$

where A_T' and C_T' are the A_T and C_T added via the salt. The term Ψ gives the non-carbonate alkalinity terms:

$$\Psi = B_T\left(\frac{K_B}{K_B + [H^+]_T}\right) + K_w[H^+]_T^{-1} - [H^+]_T + \ldots \quad (10)$$

where the ellipsis denotes terms of less importance (phosphate, silicate, indicator dye, etc.).

When addition of the salt leads to negligible change in $[H^+]_T$ without significant modification of the solution, the non-carbonate alkalinity terms (Eq. (10)) remain constant as well.

The difference between Eqs. (6) and (9) before and after a salt addition at constant $[H^+]_T$ is given by:

$$A_T' = C_T'\left(\frac{2K_1K_2 + K_1[H^+]_T}{K_1K_2 + K_1[H^+]_T + [H^+]_T^2}\right) \quad (11)$$

The C_T'/A_T' ratio of added salt is termed as Φ:

$$\Phi = \frac{C_T'}{A_T'} = \left(\frac{K_1K_2 + K_1[H^+]_T + [H^+]_T^2}{2K_1K_2 + K_1[H^+]_T}\right) \quad (12)$$

This term can be experimentally determined via laboratory procedures (Mehrbach et al., 1973).

Eq. (12) can be rearranged (Mehrbach et al., 1973) to provide a relationship in which the product of K_1 and K_2 is expressed in terms of Φ and pH:

$$K_1K_2 = \frac{10^{-2pH} + (1-\Phi)K_1 10^{-pH}}{2\Phi - 1} \quad (13)$$

This equation provides the basis for the experimental measurements in this study. A salt with an experimentally defined value of Φ is added to seawater to determine pH values at which pH remains constant within the precision of the measurement. Eq. (13) is used to determine K_2 from spectrophotometric measurements of pH and Φ in conjunction with independent experimental determinations of K_1.

A pure bicarbonate salt contributes equally to added C_T' and A_T', whereby $\Phi = 1$ ($A_T/C_T = 1$ in both the initial and the final solution). In this case, Eq. (13) reduces to the following expression:

$$pH^0_{(\Phi=1)} = 1/2(pK_1 + pK_2) \quad (14)$$

where pH^0 denotes a pH at which no pH change occurs with the addition of a specified salt (i.e., a salt with a specified Φ value). In Eq. (14), $pH^0_{(\Phi=1)}$ is the arithmetic average of pK_1 and pK_2, and this value, like all pK values, depends on S, T, and P (Mehrbach et al., 1973). At $pH^0_{(\Phi=1)}$, approximately 95% of the C_T in seawater exists as HCO_3^-, and the minor forms, CO_2* and CO_3^{2-}, have identical concentrations. Hence, the addition of pure sodium bicarbonate salt ($NaHCO_3$) to a solution at $pH^0_{(\Phi=1)}$ will not change the pH of the solution (Mehrbach et al., 1973).

3. MATERIALS

3.1. Chemicals and reagents

Natural seawater was periodically collected offshore in the Gulf of Mexico and stored in sealed flint glass carboy containers to prevent evaporation. Chemicals used in the experiments included $NaHCO_3$ (Alfa Aesar Puratronic™, 99.998% metal basis, CAS 144-55-8, Lots 25312B, T03F021, and T18F042), $KHCO_3$ (Honeywell, ≥99.95% trace metals basis, 99.7–100.5% dry basis, CAS 298-14-6, Lot MKBT3696V), and pure CO_2 gas (Air Products, anaerobe grade). Adjustments to seawater pH were made using 1 N HCl (Fisher Chemical, CAS 7647-01-0) and/or 1 N NaOH (Fisher Chemical, CAS 1310-73-2). The sulfonephthalein indicator, meta-cresol purple (mCP) (10 mM in 0.7 M NaCl), purified at the University of South Florida, was used for the spectrophotometric pH measurements (Liu et al., 2011).

3.2. Equipment

All pH measurements were carried out spectrophotometrically using a diode array spectrophotometer (Agilent 8453) with the UV lamp turned off. Sample absorbances

were measured in two-port 10 cm-cylindrical optical glass spectrophotometric cells that were periodically cleaned with HCl to prevent buildup of residue. Acid and base additions were made using Research grade PhysioCare concept pipettes (10 μL or 2.5 μL) obtained from Eppendorf Research. mCP was added with a 2 mL Gilmont micrometer buret (GS-1200). Salinity measurements were performed conductometrically with a Guildline Portasal salinometer (Model 8410) on the practical salinity scale (S_p).

A recirculating water bath (Fisher Scientific Isotemp 3013) connected to a water-jacketed cell holder inside the spectrophotometer was used to control the temperature of the spectrophotometric cells during measurements. An additional recirculating water bath (Lauda Model E100) connected to a custom-made cell warmer was used to pre-equilibrate samples in the spectrophotometric cells before measurements in the spectrophotometer. A digital handheld thermometer (Ertco-Eutechnics Model 4400) was used to measure the temperature of the cell contents (±0.025 °C) for all experiments. This handheld thermometer was calibrated against a quartz thermometer (Hewlett Packard Model 2804 A) throughout the duration of the experiments (approximately two years).

4. METHODS

4.1. Purification of solids

Following the guidelines of Kolthoff and Stenger (1964), $NaHCO_3$ and $KHCO_3$ solids were purified by bubbling a slurry of each salt (approximately 0.5–1 g) in Milli-Q water (18.2 Ω) under an atmosphere of pure CO_2 gas for several hours at room temperature. The purified solid was dried under an atmosphere of pure CO_2 gas prior to use on the same day, producing one batch of the solid. Each batch of purified solid was individually produced from the original salt Lots (provided in Section 3.1).

4.2. Spectrophotometric determinations of pH changes

The procedure for measuring pH^0 values was developed and modified from the original methods of Mehrbach et al. (1973); the major difference was our use of spectrophotometric pH measurements rather than potentiometric pH methods. The spectrophotometric measurements were made following the guidelines of Clayton and Byrne (1993) and Dickson et al. (2007). Baseline absorbance measurements were first obtained at 578 and 434 nm (absorbance maxima of the basic and acidic forms of mCP) as well as at 730 nm (a non-absorbing wavelength of mCP). After the addition of purified mCP indicator stock solution (10 μL) to the spectrophotometric cell, the cell was returned to the spectrophotometer and allowed to equilibrate for at least 30 seconds before absorbance measurements were taken again at the same three wavelengths. After small baseline corrections were made using the non-absorbing wavelength (Byrne, 1987; Clayton and Byrne, 1993; Liu et al., 2011), the ratios of absorbances at 578 and 434 nm were used to calculate seawater pH on the total scale via the mCP parameterization of Müller and Rehder (2018). The use of this mCP-based pH parameterization (rather than that of Liu et al. (2011)) facilitates future extension of the pK_2 parameterization/characterization to salinities as low as 0. It should be noted, however, that the pH^0 results obtained in our work can be used to produce pK_2 parameterizations using alternative characterizations of the physical/chemical behavior of mCP. Additionally, no dye perturbation corrections were used in this work because, for the experiments detailed in Section 4.3, it was necessary to determine the pH of the pH-adjusted seawater (using mCP) at which $NaHCO_3$ addition caused no pH change rather than characterizing the pH of the original indicator-free seawater.

The salinities of the original seawater batches (i.e., seawater periodically collected offshore) were adjusted (by evaporation or addition of Milli-Q water) to yield nine batches with salinities within the range of $19.6 \leq S_p \leq 41$. These "modified" seawater batches were prepared throughout the duration of experiments (approximately two years) immediately prior to use. Each morning, seawater from a specified "modified" seawater batch was siphoned into spectrophotometric cells (approximately 8–15 cells each day) and then pre-equilibrated for at least 30 minutes in the custom-made cell warmer to achieve a final temperature within the range of $15 \leq t \leq 35$ °C. After a preliminary pH measurement (the process of which is described in the paragraph above), the pH of each sample was iteratively adjusted with small additions of HCl or NaOH as guided by repeated spectrophotometric measurements of pH (using the same initial background absorbance values), to achieve a pH near the expected equilibrium pH^0 appropriate to the sample's S_p and T. At this point, five replicate pH measurements were made, and the average was termed $pH_{initial}$ (i.e., the pH prior to addition of $NaHCO_3$). (Because Na^+ and Cl^- are major constituents of seawater, the additions of acid and base do not significantly alter the composition of seawater, and potential impurities such as bicarbonate or carbonate in the NaOH are inconsequential because they were already present at significantly higher natural levels in the seawater samples.) Purified $NaHCO_3$ solid (approximately 0.075 g) was then added to the sample and the pH was measured again (five replicate samples), with the average providing pH_{final}. Only a small percentage of the added solid actually dissolved, and the remaining portion was allowed to quickly fall to the bottom of the spectrophotometric cell below the light path of the instrument. The temperature of the cell contents was then measured with the digital thermometer. Comparison of $pH_{initial}$ and pH_{final} established whether the sample pH increased, decreased, or did not change upon addition of $NaHCO_3$. The entire process for one sample typically took less than 30 minutes.

This procedure was then repeated using the remaining spectrophotometric cells in the cell-warmer by adjusting the $pH_{initial}$ value to be incrementally closer to the specific pH^0 value at which $NaHCO_3$ addition causes no pH change (i.e., the pH at which $pH_{final} = pH_{initial}$). The entire daily process (i.e., one set of spectrophotometric cells filled with a specific "modified" seawater batch and pH changes observed using one batch of purified $NaHCO_3$) was performed at least five times for each specified seawater

(S_p, T) pair. This process resulted in approximately 1,400 $NaHCO_3$ additions for 26 pairs of S_p and T conditions between $19.6 \leq S_p \leq 41$ and $288.15 \leq T \leq 308.15$ K.

4.3. Calculation of pH^0

When $pH > pH^0$, addition of $NaHCO_3$ would be expected to lower the sample pH. When $pH < pH^0$, that addition would be expected to increase sample pH. Values of pH^0 could thus be calculated for each of the 26 (S_p, T) pairs by determining (a) the lowest $pH_{initial}$ for which the $NaHCO_3$ addition lowered the pH (this is the lowest pH value for which $pH_{initial} > pH^0$) and (b) the highest $pH_{initial}$ for which the $NaHCO_3$ addition increased the pH (this is the highest pH value for which $pH_{initial} < pH^0$). As such, this process identified pH values very slightly greater than pH^0 and very slightly smaller than pH^0. Measurements of $pH_{initial}$ were performed with five or more batches of $NaHCO_3$ for each (S_p, T) pair until the difference between (a) and (b) was within 0.005 pH units (this process typically took around 30 samples). The average of these two $pH_{initial}$ values (which were not required to be from the same batch of $NaHCO_3$) is referred to as $pH^0_{i(avg)}$. A second pH^0 value was also calculated for each (S_p, T) pair by averaging the pH_{final} associated with observation (a) and the pH_{final} associated with observation (b). This pH_{final} average is referred to as $pH^0_{f(avg)}$. As a quality check, $pH^0_{i(avg)}$ and $pH^0_{f(avg)}$ were required to be within ± 0.001; otherwise additional measurements (i.e., using an additional set of spectrophotometric cells filled with seawater and an additional batch of purified $NaHCO_3$) were carried out until this was achieved. Finally, the overall average of the four measurements was calculated and denoted as pH^0. Thus, the calculation of each pH^0 was based on two separate sets of pH measurements (one before and one after $NaHCO_3$ addition). This pH^0 value is, as noted previously, functionally dependent on S_p and T. The resulting 26 sets of $pH_{initial}$, pH_{final}, $pH^0_{i(avg)}$, and $pH^0_{f(avg)}$ values are provided in Table A 1.1 of Appendix 1.

4.4. Assessment of $NaHCO_3$ purity (Φ)

$NaHCO_3$ (rather than the primary standard, potassium bicarbonate ($KHCO_3$)) was used in the pH^0 experiments because $NaHCO_3$ dries more rapidly than $KHCO_3$ under an atmosphere of $CO_{2(g)}$ and is therefore more convenient for daily use. Purity of the $NaHCO_3$ solid was assessed by comparison with $KHCO_3$, according to principles described in Kolthoff and Stenger (1964). Because $KHCO_3$ is a primary standard, the Φ value for this solid is, by definition, 1. Therefore, a comparison of pH^0 values obtained with $NaHCO_3$ and this primary standard will indicate any contamination of $NaHCO_3$ that needs to be accounted for. The method for assessing the purity of $NaHCO_3$ was modified from experiments described in Mehrbach et al. (1973), with these primary differences: we used natural seawater (instead of 0.72 molal NaCl) and we obtained five replicates of the purity experiments to span the salinity range between $19.6 \leq S_p \leq 41$ (rather than a single set of experiments at one salinity). A key point for the determinations of $NaHCO_3$ purity is that the same medium is used for both the $NaHCO_3$- and $KHCO_3$-based determinations of pH^0, so that the influence of the medium is removed. We used natural seawater for both.

The experiments detailed in Sections 4.2 and 4.3 were repeated with identical batches of seawater at approximately 25 °C but with added purified $KHCO_3$ rather than $NaHCO_3$. The resulting values of $pH^0_{i(avg)}$ and $pH^0_{f(avg)}$ (required to be within ± 0.001 as specified in Section 4.3) were averaged to obtain five equilibrium pH values denoted as $pH^0_{(K)}$. These five equilibrium $pH^0_{(K)}$ values were then used to calculate five pK_2 values for the $KHCO_3$ experiments, denoted as $pK_{2(K)}$, using Eq. (14). Details regarding these calculations are provided in Appendix 2, and the data are provided in Table A 2.1.

Comparisons between the experimental determinations of pH^0 (obtained via $NaHCO_3$ additions as described in Section 4.3) and $pH^0_{(K)}$ (obtained via $KHCO_3$ additions) at each specified (S_p, T) pair were used to calculate Φ (details provided in Appendix 2). Values of pH^0 were consistently larger than $pH^0_{(K)}$ (for a specified S_p, T condition), indicating the presence of Na_2CO_3 (sodium carbonate) contaminant in the $NaHCO_3$ solid, whereupon Φ will be less than 1. Salinity was identical for the corresponding pH^0 and $pH^0_{(K)}$ measurements (because a single seawater batch was used for both). The temperatures of the samples differed by no more than 0.1 °C, and T was taken as the average of the two temperature measurements. Each value of Φ was calculated via Eq. (12), using the equilibrium pH^0 values of this work, K_1 of Lueker et al. (2000), and $K_{2(K)}$ of this work. (Additional calculations of Φ using alternative K_1 parameterizations are provided in Appendix 2.)

4.5. Calculation of K_2

Eq. (13) was used to calculate stoichiometric K_2 values for bicarbonate dissociation (Mehrbach et al., 1973) at each specific (S_p, T) condition. For the required input of pH to the equation, the experimentally determined values of pH^0 were used. For the required input of K_1, two different values were used, thus generating two independent values of output K_2: one based on the K_1 parameterization of Lueker et al. (2000) (with the output here termed ${}_{SL}K_2$) and one based on the K_1 parameterization of Waters and Millero (2013) as revised by Waters et al. (2014) on the total pH scale (further referenced as Waters et al. (2013, 2014)) (with the output here termed ${}_{SW}K_2$). Calculating two independent sets of K_2 values was done to allow us to determine how the uncertainty in K_1 contributes to the calculation of K_2. This is discussed further in Section 5.2.

4.6. Deviations from K_1K_2 methods of previous works

The procedures used in the present study are in certain respects distinct from the procedures of Mehrbach et al. (1973) and of Mojica Prieto and Millero (2002). One difference is our use of purified $NaHCO_3$ in pH^0 experiments (as described in Section 4.1). In the experiments of Mehrbach et al. (1973), the $KHCO_3$ solid was purified in a similar manner as described in Section 4.1. However, as no

mention was made of purification techniques for $NaHCO_3$, we infer that the sodium bicarbonate used in their work (Mehrbach et al., 1973) was not purified. The $NaHCO_3$ solid used by Mojica Prieto and Millero (2002) was likewise unpurified. To determine the purity of the $NaHCO_3$ solid, Mojica Prieto and Millero (2002) directly measured the C_T and A_T of a 0.7 M NaCl solution to which $NaHCO_3$ had been added. The background NaCl solution likely had non-zero A_T and C_T, and the $KHCO_3$ reference method of Mehrbach et al. (1973) was not utilized.

Another major deviation from the procedures of Mehrbach et al. (1973) and Mojica Prieto and Millero (2002) was our use of single $NaHCO_3$ additions to determine pH^0. Mehrbach et al. (1973) used multiple $NaHCO_3$ additions to alkalinity-free seawater to reach a potentiometrically measured steady-state pH. We opted not to use multiple additions because these additions alter the seawater composition, changing the sodium concentration and ionic strength and potentially titrating acid/base species. Furthermore, we chose to work with solution compositions as close as possible to natural seawater and therefore we did not drive off $CO_{2(g)}$ to create alkalinity-free waters beforehand. (Whether this methodological difference is consequential is difficult to assess.) Mehrbach et al. (1973) made additions of $NaHCO_3$ from both the acidic and basic sides of pH^0, whereas Mojica Prieto and Millero (2002) approached the final steady-state pH only from the acidic side. In our work, $pH_{initial}$ and pH_{final} values obtained before and after single $NaHCO_3$ additions were used to identify the equilibrium pH for a given (S_p, T) condition (as described in Section 4.3).

Mehrbach et al. (1973) and Mojica Prieto and Millero (2002) both determined steady-state pH by potentiometric measurements. The latter authors additionally measured the final steady-state pH values spectrophotometrically, but unpurified mCP was used because purified indicator was not available at the time. The present work used purified mCP and state-of-the-art spectrophotometric techniques.

4.7. CO_2 system calculations

Internal consistency was assessed by comparing measured and calculated values of CO_2 system parameters (i.e., calculated using different sets of dissociation constants). Differences between measured and calculated values of X are referred to as residuals of X (e.g., A_T residuals = A_T measured – A_T calculated). The CO_2 system calculations were made using the CO2SYS-MATLAB software, version 2.0 (Lewis and Wallace, 1998; van Heuven et al., 2011). All pH calculations were carried out on the total hydrogen ion concentration scale unless otherwise specified. Values for K_{HSO4} from Dickson (1990) and B_T/S from Lee et al. (2010) were used. The CO_2 dissociation constants for each calculation were explicitly specified using the following notation: constants of Lueker et al. (2000) are denoted as "$_LK$", and constants of Waters et al. (2013, 2014) on the total pH scale are denoted as "$_WK$". The K_2 parameterization produced in this work is denoted as "$_{SW}K_2$". This K_2 parameterization will be discussed further in Section 5.1. CO2SYSv3 in MATLAB, developed by Sharp et al. (2020), includes the $_{SW}K_2$ parameterization of this work as an option for calculations (for details see Appendix 3).

4.8. Data sets for internal consistency assessments

Internal consistency of the CO_2 system calculations was assessed by using the newly obtained K_2 parameterization to generate calculated parameters that were then compared to measured parameters in two high-quality data sets: (1) the original experimental data set of Lueker et al. (2000) and (2) a compilation of nine large oceanic data sets in which three or more CO_2 system parameters had been measured using state-of-the-art techniques.

The data from Lueker et al. (2000) consisted of paired measurements of fCO_2, A_T, and C_T made on the same seawater sample over a range of fCO_2. The fCO_2 measurements were largely obtained over the ranges of $34.966 \leq S_p \leq 36.643$ and $15 \leq t \leq 25$ °C ($n = 51$). Five additional measurements made at 5 °C were excluded from our analysis because this temperature is well below the range investigated in our work.

The field data were obtained from a suite of repeat hydrography cruises ($n = 21{,}475$). These data sets were chosen to represent a wide range of oceanographic conditions throughout the major ocean basins. The National Oceanographic Data Center expedition codes (EXPOCODES) for these cruises are as follows: 32WC20110812 (West Coast Ocean Acidification Cruise (WCOA) 2011) (Feely et al., 2016), 33AT20120419 (A20 2012) (Wanninkhof et al., 2013), 33RO20120721 (Gulf of Mexico and East Coast Carbon Cruise 2 (GOMECC-2) 2012) (Wanninkhof et al., 2016), 318M20130321 (P02 2013) (Swift et al., 2014), 320620140320 (P16S 2014) (Talley et al., 2016), 33RO20150410 and 33RO20150525 (P16N 2015) (Cross et al., 2017), 33RR20160208 (I08S 2016) (Macdonald et al., 2018), 33RR20160321 (I09N 2016) (Barbero et al., 2018), and 33RO20161119 (P18 2016) (Carter et al., 2018). Full profiles of A_T, C_T, pH, T, S, P, silicate, and soluble reactive phosphate were measured for all data sets. Data records with flags indicating poor quality were removed prior to analysis. In most cases, pH was measured spectrophotometrically onboard using purified mCP, on the total hydrogen ion concentration scale, at temperatures of approximately 25 °C. Exceptions were P18 2016 (where pH was measured on the SWS scale) and P16S 2014 (where pH was measured at 20 °C). For all cruises, accuracies of the onboard A_T and C_T measurements were assessed using certified reference materials (CRMs) provided by the laboratory of Dr. Andrew Dickson at Scripps Institution of Oceanography. All of the cruise data can be found online at the website of the NOAA National Centers for Environmental Information (https://www.nodc.noaa.gov/ocads/oceans/RepeatSections/).

5. RESULTS

5.1. Stoichiometric pK_2 parameterizations and residuals

The purity of the $NaHCO_3$ used in the K_2 determinations was determined as described in Section 4.4, using the experimental values of $pH^0_{i(avg)}$ and $pH^0_{f(avg)}$ in Eq. (12). These values of Φ, as well as the average Φ for each set of calculations, are provided in Table A 2.2 of Appendix 2. The purity of the $NaHCO_3$ used in this work is given by $\Phi = 0.9996 \pm 0.0003$. This value compares well to the value reported in Mehrbach et al. (1973), $\Phi = 0.9991 \pm 0.0002$.

Two sets of pK_2 values were determined as described in Section 4.5, using the experimentally derived pH^0 values and either the K_1 of Lueker et al. (2000) or the K_1 of Waters et al. (2013, 2014). The two sets of values, denoted as $_{SL}pK_2$ and $_{SW}pK_2$, are provided in Table 1. These two sets of pK_2 values agree remarkably well with one another. The largest difference between $_{SL}pK_2$ and $_{SW}pK_2$ values is 0.007, which is less than the uncertainty associated with the determinations of K_2.

Because the Waters K_1 results are appropriate over a wider range of salinity and temperature than Lueker et al. (2000), we elected to rely primarily on the K_1 description of Waters et al. (2013, 2014) for our parameterization of K_2. The S_p and T dependences of the resulting $_{SW}pK_2$ values are shown in Fig. 1 as a function of T^{-1}. The $_{SW}pK_2$ values given in Table 1 were parameterized using Eq. (15):

$$pK_2 = e_1 + e_2T^{-1} + e_3\ln T + e_4S_p + e_5S_p^{0.5} + e_6S_p^{2} + e_7(S_p/T) \quad (15)$$

The e_n coefficients for this parameterization are given in Table 2. Eq. (15) is based on the original pK_2 parameterization of Lueker et al. (2000), with additional terms ($S_p^{0.5}$ and S_p/T) included based on an F-test to more appropriately represent the data. The root mean square error (RMSE) of $_{SW}pK_2$ is 0.0029.

Residuals for the $_{SW}pK_2$ parameterization (i.e., parameterized minus experimental values) are shown in Fig. 2. The standard deviation of the residuals is 0.0029, and all residuals are randomly distributed with respect to both S_p and T.

The set of $_{SL}pK_2$ values calculated using the K_1 of Lueker et al. (2000), also parameterized as described in this section (Section 5.1), is given in Appendix 4 along with the corresponding e_n coefficients. Differences between the parameterizations of $_{SL}pK_2$ and $_{SW}pK_2$ and, as well, the closely linked pK_1 characterizations of Lueker et al. (2000) and Waters et al. (2013, 2014) are shown in Fig. 3 in terms of S_p and T.

5.2. Estimating uncertainties

The pooled standard deviation in measurements of pH^0 was calculated to be 0.0013 (individual standard deviations

Table 1
Experimentally derived pH^0 values and associated standard deviations for a range of salinity and temperature conditions. The uncertainty of the listed temperatures is ± 0.02 °C. The pH^0 values for each (S_p, T) pair were averaged from the two pH_{intial} and two pH_{final} values (provided in Table A 1.1). Also shown are the two sets of pK_2 values calculated using the K_1 parameterizations of Lueker et al. (2000) (denoted as $_{SL}pK_2$) and Waters et al. (2013, 2014) (denoted as $_{SW}pK_2$).

S_p	t (°C)	pH^0 (±stdev) ($n = 4$)	$_{SL}pK_2$	$_{SW}pK_2$
19.62	15.19	7.6605 ± 0.0024	9.2938	9.3000
19.62	20.03	7.6045 ± 0.0012	9.2289	9.2354
19.62	25.05	7.5443 ± 0.0015	9.1532	9.1596
19.62	29.93	7.4857 ± 0.0011	9.0754	9.0817
19.62	34.81	7.4297 ± 0.0008	8.9992	9.0053
24.70	15.24	7.6096 ± 0.0018	9.2257	9.2258
24.70	20.11	7.5477 ± 0.0014	9.1494	9.1502
24.70	25.07	7.4869 ± 0.0009	9.0718	9.0734
26.51	29.65	7.4145 ± 0.0009	8.9743	8.9754
26.51	34.65	7.3583 ± 0.0007	8.8987	8.9013
29.11	20.07	7.5154 ± 0.0007	9.1082	9.1048
29.11	24.99	7.4528 ± 0.0009	9.0266	9.0246
29.11	29.95	7.3932 ± 0.0015	8.9475	8.9471
31.70	15.35	7.5511 ± 0.0015	9.1456	9.1397
31.70	34.69	7.3125 ± 0.0013	8.8327	8.8336
35.50	15.43	7.5269 ± 0.0018	9.1126	9.1061
35.50	20.36	7.4627 ± 0.0010	9.0321	9.0266
36.33	25.10	7.3979 ± 0.0007	8.9472	8.9437
36.33	30.08	7.3374 ± 0.0011	8.8662	8.8653
36.33	35.02	7.2778 ± 0.0012	8.7831	8.7853
36.80	25.00	7.3992 ± 0.0010	8.9503	8.9470
40.98	15.05	7.5007 ± 0.0029	9.0717	9.0685
40.98	20.05	7.4319 ± 0.0009	8.9829	8.9808
40.98	25.09	7.3697 ± 0.0009	8.9032	8.9031
40.98	29.89	7.3101 ± 0.0009	8.8228	8.8255
40.98	34.88	7.2471 ± 0.0013	8.7332	8.7397

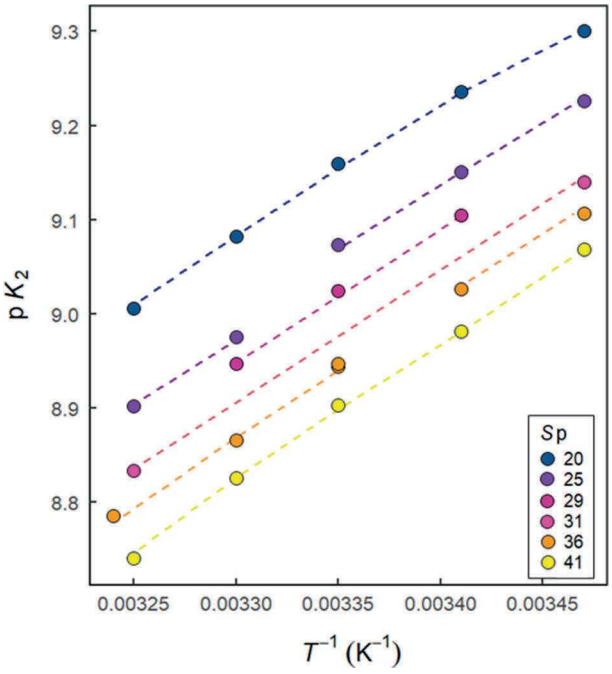

Fig. 1. Experimentally derived $_{SW}pK_2$ values as a function of inverse temperature (K^{-1}), with colors indicating approximate salinity. The dashed lines show the $_{SW}pK_2$ parameterization of Eq. (15).

Table 2
Coefficients for the $_{SW}pK_2$ parameterization of Eq. (15) calculated using the K_1 of Waters et al. (2013, 2014). As a check, the value at $S_p = 35$ and $T = 298.15$ K is $_{SW}pK_2 = 8.9608$.

$pK_2 = e_1 + e_2T^{-1} + e_3 \ln T + e_4S_p + e_5S_p^{0.5} + e_6S_p^2 + e_7(S_p/T)$

	$_{SW}pK_2$
e_1	116.8067
e_2	–3655.02
e_3	–16.45817
e_4	0.04523
e_5	–0.615
e_6	–0.0002799
e_7	4.969

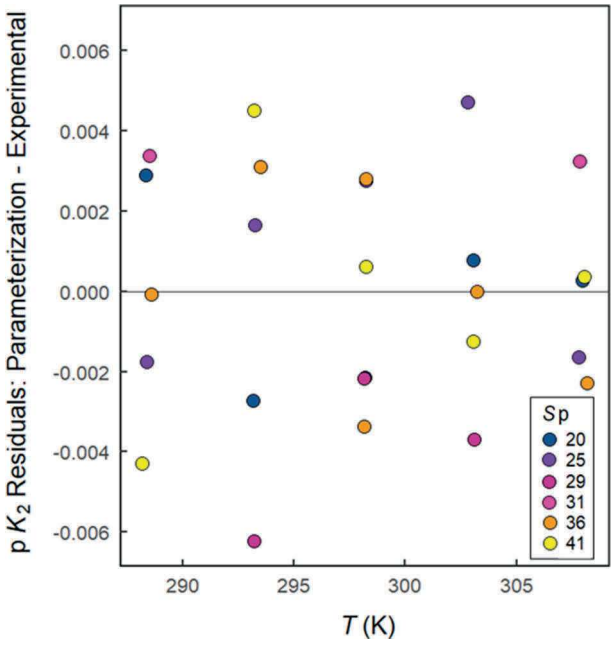

Fig. 2. $_{SW}pK_2$ residuals (i.e., parameterized pK_2 minus experimental pK_2) as a function of temperature (K), with colors indicating approximate salinity.

are provided in Table 1). To further assess the uncertainty in our original measurements of pH^0 and associated p(K_1K_2) values (calculated with the K_1 of Waters et al. (2013, 2014)) (provided in Table A 4.1 of Appendix 4), both were fitted using Eq. (15). The e_n coefficients are given in Table A 4.2 of Appendix 4. The root mean square error for pH^0 is 0.0014 and for p(K_1K_2) is 0.0028. Because our method requires the use of previous K_1 parameterizations, any estimated uncertainty in K_1 will influence the uncertainty in our K_2 parameterization. The uncertainty in pK_1 is 0.0075 according to Orr et al. (2018) which, as shown in Fig. 3b, is the approximate magnitude of the difference between our pK_2 parameterizations ($_{SL}pK_2$ and $_{SW}pK_2$). Notably, as shown in Fig. 3, systematic overestimates in a utilized K_1 parameterization will produce underestimates in the conjugate K_2 parameterization. Our estimates of K_2 are also influenced by the assumption that $KHCO_3$ is completely pure (i.e., $\Phi = 1$). Any systematic deviation from this assumption will, of course, lead to systematic errors in calculations of K_1K_2. It is not possible, at present, to quantify this potential source of error.

Estimates of uncertainty in pK_2 were assessed by a method similar to that of Orr et al. (2018). Based on the pK_2 parameterizations obtained (a) in this work ($_{SW}pK_2$), (b) by Lueker et al. (2000), and (c) by Waters et al. (2013, 2014), estimates of systematic uncertainty in pK_2 were assessed to be on the order of ±0.01. Random uncertainty in pK_2 was estimated based on the standard deviation of the pK_2 residuals. For this work, the estimated random uncertainty is 0.003, which is less than a third of the 0.01 uncertainty estimated by Orr et al. (2018) for the pK_2 parameterization of Lueker et al. (2000). The total standard uncertainty for pK_2 (based on the combined random and systematic components of uncertainty) for this work is 0.010. The total standard uncertainty estimated by Orr et al. (2018) for previous parameterizations of pK_2 is 0.015.

6. DISCUSSION

6.1. Comparison with other pK_2 parameterizations

In Fig. 4, the pK_2 residuals for this work (i.e., $_{SW}pK_2$ – pK_2 experimental) are compared to the residuals of other recent parameterizations. The pK_2 residuals of this work (Fig. 4a) are more tightly and evenly distributed about zero than are the residuals of Lueker et al. (2000) and Millero et al. (2006) (Fig. 4b and c). This result affirms the improved pK_2 precision that can be obtained using the methods described in Section 4. Notably, Fig. 4b and 4c show that the residuals of Lueker et al. (2000) and Millero et al. (2006) are not randomly distributed with respect to S_p and T. In an attempt to obtain improved residuals, we refit the original data from these two studies to parameterizations with fewer terms and additional terms, but the uneven distributions of residuals remained.

The $_{SW}pK_2$ parameterization obtained in this work was compared to the pK_2 parameterizations of Lueker et al. (2000) and Waters et al. (2013, 2014). Fig. 5 shows differences in terms of $\Delta pK_2 = {}_{SW}pK_2$ (this work) – pK_2 (Lueker or Waters). For $25 \le S_p \le 41$, the best agreement between $_{SW}pK_2$ and the pK_2 of Lueker et al. (2000) or Waters et al. (2013, 2014) is generally seen within the temperature range of $20 \le t \le 30$ °C, where the range of ΔpK_2 is ≤ 0.02, with a slight negative offset. At higher and lower temperatures, the range of ΔpK_2 has a slightly larger negative offset. At the lowest salinity ($S_p = 20$), ΔpK_2 is typically positive over the entire range of temperatures, with the largest ΔpK_2 being observed between $25 \le t \le 30$ °C. Overall, although $_{SW}pK_2$ is based in part on the pK_1 of Waters et al. (2013, 2014), better agreement is observed with the pK_2 parameterization of Lueker et al. (2000) over the range of temperatures considered in this work.

Differences between $_{SL}pK_2$ and the pK_2 parameterizations of Lueker et al. (2000) and Waters et al. (2013, 2014) are similar to those described above for $_{SW}pK_2$. Agreement is best within the range $20 \le t \le 30$ °C with larger differences being observed at higher and lower temper-

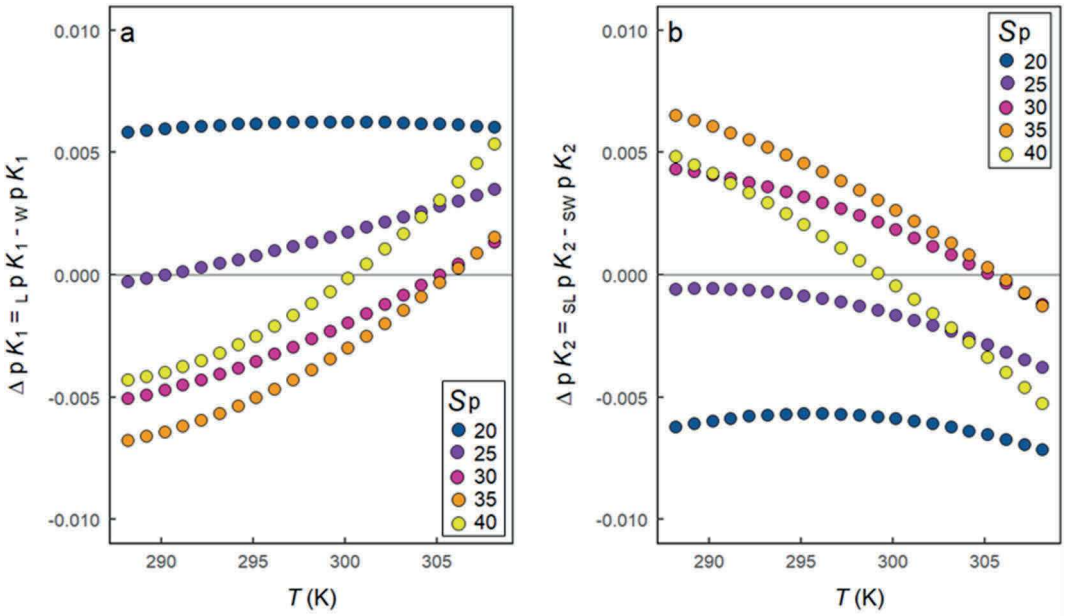

Fig. 3. Differences between pK parameterizations as a function of temperature (K), color-coded by salinity for (a): $\Delta pK_1 = pK_1$ of Lueker et al. (2000) minus pK_1 of Waters et al. (2013, 2014) and (b) $\Delta pK_2 = {}_{SL}pK_2$ minus ${}_{SW}pK_2$.

atures (not shown). The agreement of ${}_{SL}K_2$ and ${}_{SW}K_2$ with both Lueker et al. (2000) and Waters et al. (2013, 2014) is significant because ${}_{SL}K_2$ and ${}_{SW}K_2$ are derived from different K_1 parameterizations. Because, as noted previously, the pK_1 parameterization of Waters et al. (2013, 2014) extends to much lower salinities than the pK_1 of Lueker et al. (2000), the Waters parameterization can be used in future K_1K_2 determinations to extend ${}_{SW}pK_2$ to a much wider range of salinity conditions.

6.2. Assessments of internal consistency

6.2.1. Lueker et al. (2000) data set: fCO_2, A_T, and C_T

One assessment of internal consistency was conducted using the original experimental data of Lueker et al. (2000) ($n = 47$), in combination with the sets of dissociation constants introduced in Section 4.7: set A = ${}_{L}K_1$ and ${}_{L}K_2$ (the constants of Lueker et al. (2000)), set B = ${}_{W}K_1$ and ${}_{W}K_2$ (the constants of Waters et al. (2013, 2014)), and set C = ${}_{W}K_1$ and ${}_{SW}K_2$ of this work. Summary statistics of the resulting relative residuals of fCO_2 (i.e., (fCO_2 measured – fCO_2 calculated), expressed as a percentage of the calculated fCO_2 value) are listed in Table 3. (All residuals are provided in Table A 5.1 of Appendix 5.)

For all sets of dissociation constants, the mean relative residuals for $fCO_2 < 500$ µatm (characterized as "low-fCO_2 conditions") are negative. For $fCO_2 > 500$ µatm (characterized as "high-fCO_2 conditions"), the mean relative residuals calculated using set C are internally consistent within the uncertainty of measurements, while those calculated using sets A and B are both positive. For both low- and high-fCO_2 conditions, these two sets of mean relative residuals are not significantly different from one another at the 95% confidence level. In contrast, for both low- and high-fCO_2 conditions, the mean relative residuals of set C (i.e., ${}_{SW}pK_2$ of this work) are significantly different from those of sets A and B at the 95% confidence level. Overall, the mean relative fCO_2 residuals for all constants at low-fCO_2 conditions show that observations and predictions (calculated values) are not internally consistent within the uncertainty of measurements (i.e., the mean ±95% confidence intervals do not include zero for any sets of constants). Thus, there are clear differences in the degree of internal consistency based on the choice of CO_2 system dissociation constants. Under high-fCO_2 conditions, only the parameterization of the set C constants provides internally consistent observations and predictions.

Calculations of fCO_2 were also made using the B_T/S of Uppström (1974). In this case, compared to residuals calculated using the B_T/S of Lee et al. (2010), the mean residuals for low-fCO_2 conditions are increased by approximately 5 µatm while the mean residuals for high-fCO_2 conditions are increased by approximately 11 µatm for calculations with all three sets of K_1 and K_2 constants. Mean residuals calculated with the B_T/S of Uppström (1974) therefore prompt different interpretations with respect to which sets of dissociation constants provide the most internally consistent results. The mean residuals at low-fCO_2 become closer to zero (i.e., more internally consistent) for sets A and C, while the mean residuals at high-fCO_2 move farther from zero (i.e., less internally consistent) for all sets of constants. The choice of parameterization for B_T/S will clearly influence interpretations regarding which calculations are internally consistent.

6.2.2. Cruise data sets: A_T, C_T, and pH_T

A second assessment of internal consistency was conducted using the cruise data described in Section 4.8 ($n = 21{,}475$) in combination with the three sets of dissociation constants listed in Section 6.2.1. The measured param-

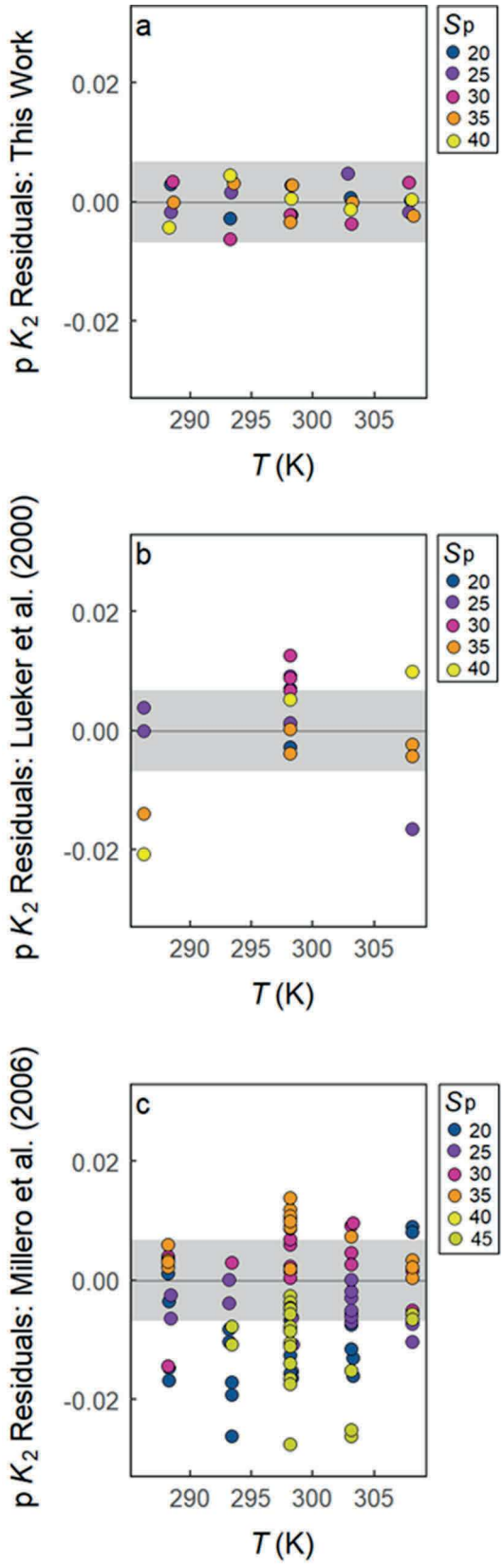

Fig. 4. pK_2 residuals (i.e., parameterized pK_2 minus experimental pK_2) as a function of temperature (within the range of $288.15 \leq T \leq 308.15$ K), color-coded by salinity for: (a) this work's $_{SW}pK_2$, (b) Lueker et al. (2000), and (c) Millero et al. (2006) (which provide the experimental basis for the Waters constants). For ease of comparison, the gray shaded region shows ± two standard deviations for the residuals of this work (±0.0068). Data were grouped by S_p in increments of five and therefore color indicates approximate salinity. Thus, for example, S_p of 30 denotes data obtained within the range of 30 ± 2.5.

eters used were A_T, C_T, and pH_T (pH_{SWS} was used only for P18 2016). The mean residuals of A_T for all cruises (Fig. 6) are generally within the ±10 μmol kg^{-1} measurement uncertainty (95% confidence interval) of a single at-sea A_T measurement (McLaughlin et al., 2015). When the set A (Lueker) or set C (this work) characterizations are used, the mean residuals generally provide internally consistent results. When the set B (Waters) constants are used, however, the mean residuals for five of the nine cruises are offset from zero by more than one standard deviation, with an average mean A_T residual (nine cruises) of approximately 4 μmol kg^{-1} (Table A 5.2 of Appendix 5). For the P16N 2015 cruise, only the mean A_T residuals calculated using $_{SW}pK_2$ (i.e., Set C) provide internally consistent results, whereas the mean A_T residuals calculated with both Lueker et al. (2000) and Waters et al. (2013, 2014) are offset from zero by more than one standard deviation. The mean residuals of C_T (not shown) displayed similar patterns to the mean A_T residuals but with opposite sign, as would be expected. For pH assessments, when the set A (Lueker) or set C (this work) characterizations are used, the mean residuals generally provide internally consistent results, whereas mean residuals calculated with set B (Waters) are generally offset from zero by more than one standard deviation (Table A 5.3 of Appendix 5). The K_{HSO4} of Waters et al. (2013, 2014) was also used in CO_2 system calculations and produced no meaningful changes in the internal consistency assessments described in this section (which uses the K_{HSO4} of Dickson (1990)).

Whereas this type of analysis (i.e., comparisons of mean residuals) provides a simple way to assess the degree of internal consistency across sets of dissociation constants (with all other parameter uncertainties being held constant), it is recognized that such comparisons provide only limited insight into the accuracy. As a note of caution, although the Lueker et al. (2000) K_1 and K_2 parameterizations appear to yield better internal consistency than the parameterizations of Waters et al. (2013, 2014), it must be noted that the A_T measurements in Fig. 6 likely include contributions from organic bases (Kim and Lee, 2009; Sharp and Byrne, 2020). If these contributions were appropriately accounted for, the calculated values of A_T would be increased, thus potentially reducing the mean offsets calculated here. If organic contributions were sufficiently large, the most positive residuals in Fig. 6 could become considerably smaller and the residuals now near zero could become negative. As such, with improved accounts of organic alkalinity distributions in

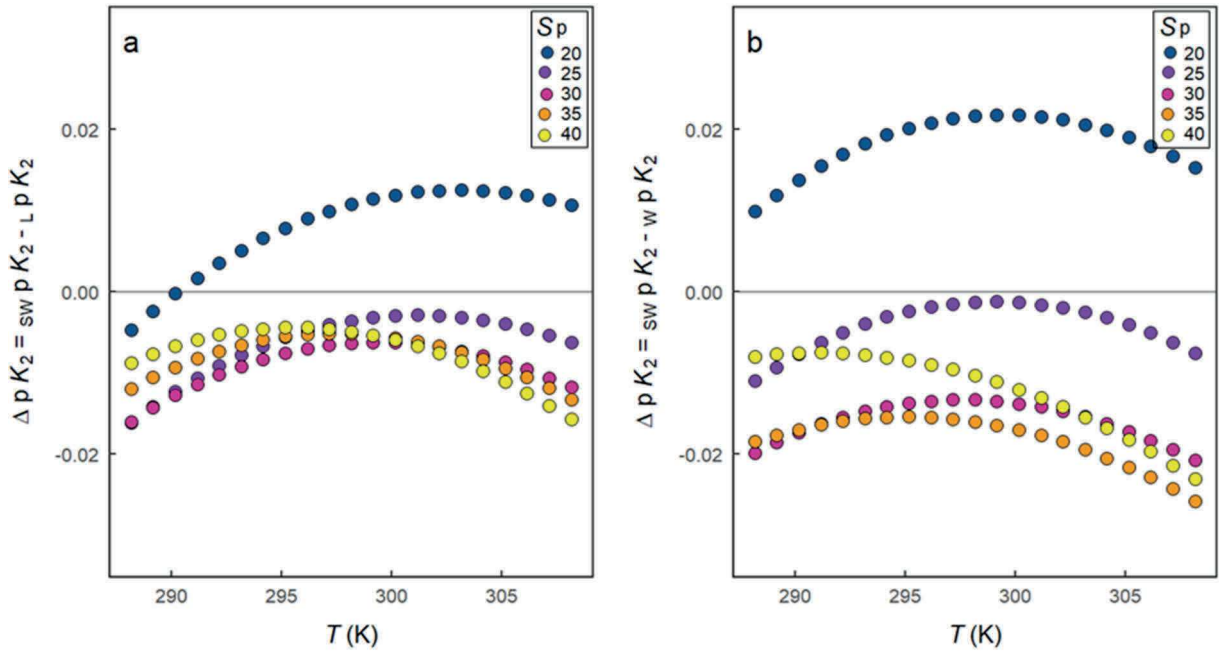

Fig. 5. Differences between the ${}_{SW}pK_2$ parameterization of this work and the pK_2 parameterizations of (a) Lueker et al. (2000) (${}_{L}pK_2$) and (b) Waters et al. (2013, 2014) (${}_{W}pK_2$) as a function of temperature (K), color-coded by salinity.

Table 3
Mean relative fCO_2 residuals ((fCO_2 measured – fCO_2 calculated)/fCO_2 calculated) calculated using the different sets of K_1 and K_2 listed in the left column with the experimental fCO_2, A_T, and C_T data of Lueker et al. (2000) (excluding their data collected at 5 °C*). Uncertainty is given as the 95% confidence interval on the mean.

Constants	Mean relative fCO_2 residuals ± uncertainty (%)	
	$fCO_2 < 500$ µatm ($n = 28$)	$fCO_2 > 500$ µatm ($n = 19$)
Set A = Lueker ${}_{L}K_1$ and ${}_{L}K_2$	−1.27 ± 0.33	1.37 ± 0.93
Set B = Waters ${}_{W}K_1$ and ${}_{W}K_2$	−0.64 ± 0.36	1.97 ± 0.89
Set C = Waters ${}_{W}K_1$ and this work ${}_{SW}K_2$	–2.93 ± 0.35	0.01 ± 0.86

*Data also excludes four points that were excluded from Fig. 4b of Lueker et al. (2000).

the ocean, the internal consistency evaluation shown in Fig. 6 could be significantly revised.

7. CONCLUSIONS AND IMPLICATIONS

This study provides significant improvements in the characterization of K_2, the stoichiometric dissociation constant of bicarbonate. As shown in Fig. 4, the calculated residuals for ${}_{SW}pK_2$ are randomly distributed and are substantially smaller than those obtained in previous studies. This result indicates that our new method reduces the likelihood of systematic errors in pK_2 that vary with temperature and salinity. Furthermore, if future studies improve the characterization of K_1, the original experimental pH^0 data summarized in Table 1 (and parameterized in Table A 4.2 of Appendix 4) can be used to recalculate K_2. The ${}_{SW}pK_2$ parameterization developed in this work (using the K_1 parameterization of Waters et al. (2013, 2014)) agrees well with the pK_2 dissociation constant parameterizations of both Lueker et al. (2000) and Waters et al. (2013, 2014) within the ranges of $25 \leq S_p \leq 41$ and $20 \leq t \leq 30$ °C. Nevertheless, there are pronounced differences at low salinities and at higher and lower temperatures.

In previous determinations of CO_2 system dissociation constants, assessments of the quality of the experimental K_1 and K_2 results have typically been limited to direct comparisons with earlier K_1 and K_2 parameterizations. In this work, we evaluated our new pK_2 parameterization by making similar historical comparisons and, in addition, by conducting internal consistency assessments that relied on two independent and extensive data sets: (a) the fCO_2, A_T, and C_T data set of Lueker et al. (2000) and (b) the A_T, C_T, and pH data sets from nine ocean research cruises. Assessments based on the Lueker data set show that calculations made with the ${}_{SW}K_2$ parameterization of this work perform as well as or better than calculations carried out with the constants of Lueker et al. (2000) or Waters et al. (2013, 2014).

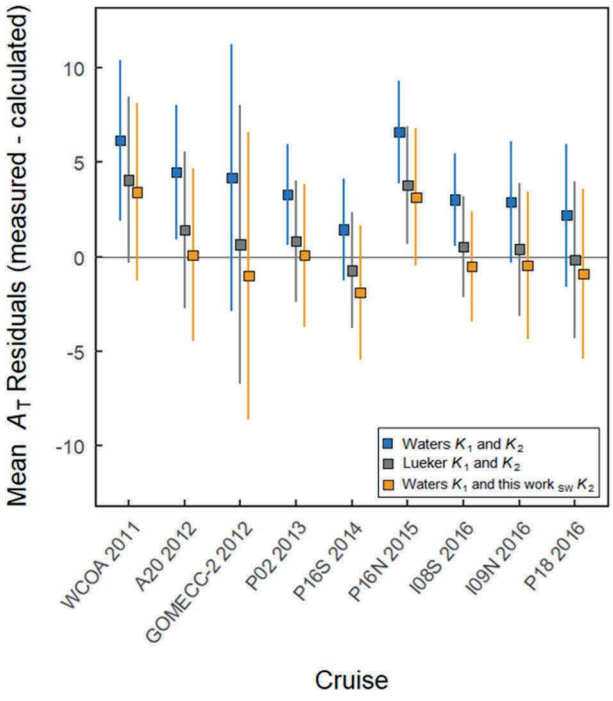

Fig. 6. Average residuals (measured – calculated) of A_T (μmol kg^{-1}) for the nine cruise data sets calculated using the three sets of dissociation constants (shown in colors). Standard deviations are shown by the colored bars.

Assessments based on the large oceanographic data sets show that A_T residuals calculated using $_{SW}K_2$ compared well with calculations that used the Lueker et al. (2000) dissociation constants. Based on these results we recommend, for the salinity and temperature ranges of $19.6 \leq S_p \leq 41$ and $15 \leq t \leq 35$ °C, the use of $_{SW}pK_2$ (Eq. (15) and Table 2) paired with the pK_1 of Waters et al. (2013, 2014) on the total pH scale.

Internal consistency assessments constitute an important tool for comparing K_2 parameterizations, but the available data cover only a small range of environmentally relevant S and T. Most of the Lueker et al. (2000) laboratory data encompass a small range of temperature (approximately 15–25 °C), all at salinities near 36. The oceanographic (cruise) data cover a wider range of salinities, but nearly all at 25 °C. Additional internal consistency comparisons should be obtained over wider ranges of S and T. It would be very useful, for example, if measurements of A_T and C_T could be combined with pH_T and high quality fCO_2 measurements obtained over a wide range of temperatures to better identify likely causes of calculated discrepancies. This extension is important because the internal consistency assessments in this work are largely made at a temperature (25 °C) where $_{SW}pK_2$ and the pK_2 parameterizations of Lueker et al. (2000) and Waters et al. (2013, 2014) most closely agree. At lower temperatures, where the pK_2 parameterizations show larger differences (see Fig. 5), less agreement in internal consistency assessments would be expected. An expanded range of temperatures in evaluations of A_T, C_T, and pH_T internal consistency could also help to address discrepancies between in-situ measurements and calculated in-situ CO_2 system parameters, including calcium carbonate saturation states (Ω) (Naviaux et al., 2019).

Experimental determinations of K_1K_2 should be expanded to extend the K_2 parameterization to estuarine conditions. Notably, the K_1 of Lueker et al. (2000) is valid only within the range $19 \leq S_p \leq 43$, but the K_1 of Waters et al. (2013, 2014) is appropriate for $0 \leq S_p \leq 45$. As noted in Section 6.1, the two pK_2 parameterizations obtained in the present work (one based on the pK_1 parameterization of Lueker et al. (2000) and the other based on that of Waters et al. (2013, 2014)) are in good agreement. Therefore, it is expected that future determinations of K_1K_2 for estuarine conditions, in conjunction with the K_1 of Waters et al. (2013, 2014), could be directly combined with the results of this work to obtain an accurate pK_2 parameterization that encompasses both estuarine and marine conditions.

The accuracy of pK determinations is most reliably assessed through comparisons of results obtained by independent investigators who, ideally, used dissimilar measurement procedures. Based on such criteria, it is difficult to quantitatively assess the absolute accuracy of the pK characterizations obtained in the present study. As noted above, evaluations of internal consistency are useful but are narrow in scope. Assessments of accuracy are currently limited by uncertainties such as (unknown) organic base contributions to A_T and uncertainty in the B_T/S ratio. Nevertheless, it is possible to make useful statements about what does and does not contribute to systematic errors in determinations of pK and characterizations of the marine carbonate system.

Because the pK_2 parameterization obtained in our work was derived using the pK_1 parameterization of Waters et al. (2013, 2014), any errors inherent in this parameterization will be propagated to $_{SW}pK_2$. It should be noted that, via Eq. (14), K_1 and K_2 are anti-correlated (i.e., overestimates of $_WK_1$ will produce underestimates of $_{SW}K_2$ and vice versa). The quantitative relationship between pK_1 and pK_2 given in Eq. (14) can be used to explore the influence of pK_1 perturbations on internal consistency evaluations (e.g., Table 3 and Fig. 6).

The determinations of pH in this work are based on the mCP parameterization of Müller and Rehder (2018). Examination of Eq. (14) shows that the accuracy of the $\log(K_1K_2)$ characterizations is intimately (directly) related to the accuracy of the pH characterizations. For example, if the pH parameterization of Müller and Rehder (2018) is in error by $+0.01$ then $1/2\log(K_1K_2)$ will be in error by an identical offset. Nevertheless, as an important point, the combination of these directly correlated errors should provide an accurate depiction of $[CO_3^{2-}]_T/[CO_2^*]$ ratios (i.e., $[CO_3^{2-}]_T/[CO_2^*] = K_1K_2/[H^+]_T^2$ with offsetting errors in K_1K_2 and $[H^+]_T^2$). Thus, whereas errors in spectrophotometric pH parameterizations will produce corresponding errors in $\log(K_1K_2)$, the accuracy of carbonate system characterizations will not be affected. In this sense, the accuracy of CO_2 system calculations is maintained even in the presence of some types of systematic errors. An important point

here is that, due to correlation of errors in measured pH and parameterized pK, the pK results in this work should best be paired with the mCP (pH) parameterization of Müller and Rehder (2018). Other pH parameterizations could be used, but only after the pK results in the present work are recalculated and made compatible with the alternative pH model (e.g., Liu et al., 2011).

Declaration of Competing Interest

The authors declare that they have no known competing financial interests or personal relationships that could have appeared to influence the work reported in this paper.

ACKNOWLEDGEMENTS

This work was supported by the Paul L. Getting Memorial Fellowship in Marine Science and the St. Petersburg Downtown Partnership Endowed Fellowship in Coastal Science (University of South Florida College of Marine Science), the U.S. Geological Survey, and the National Science Foundation [grant number OCE-1657894]. We would like to sincerely thank Dr. Tonya Clayton for editorial assistance and guidance in improving the manuscript. We would also like to thank Dr. Alfonso Mucci, Dr. Andrew Dickson, and two anonymous reviewers whose constructive comments greatly improved the final work.

ROLE OF FUNDING SOURCE

Funding sources of this work include the University of South Florida College of Marine Science, the U.S. Geological Survey, and the National Science Foundation [grant number OCE-1657894]. These sources provided financial support for conducting research and preparation of the article but had no other involvement.

APPENDIX A. SUPPLEMENTARY MATERIAL

Supplementary data to this article can be found online at https://doi.org/10.1016/j.gca.2021.02.008.

REFERENCES

Barbero L., Wanninkhof R., Dickson A. G., Carlson C. A., Key R. M., Becker S., Swift J. H., McNichol A. and Rodriguez C. (2018) Discrete profile measurements of dissolved inorganic carbon, total alkalinity, pH on total scale and other hydrographic and chemical data obtained during the R/V Roger Revelle Repeat Hydrography Cruise in the Indian Ocean: GO-SHIP Section I09N, (EXPOCODE 33RR20160321) from 2016–03-21 to 2016–04-28 (NCEI Accession 0178637). NOAA National Centers for Environmental Information, Dataset https://doi.org/10.25921/f59c-dy18.

Bates N. R., Astor Y. M., Church M. J., Currie K., Dore J. E., Gonzalez-Davila M., Lorenzoni L., Muller-Karger F., Olafsson J. and Santana-Casiano J. M. (2014) A time-series view of changing surface ocean chemistry due to ocean uptake of anthropogenic CO_2 and ocean acidification. *Oceanography* **27**, 126–141. https://doi.org/10.5670/oceanog.2014.16.

Byrne R. H. (1987) Standardization of standard buffers by visible spectrometry. *Anal. Chem.* **59**, 1479–1481. https://doi.org/10.1021/ac00137a025.

Byrne R. H. (2014) Measuring ocean acidification: new technology for a new era of ocean chemistry. *Environ. Sci. Technol.* **48**, 5352–5360. https://doi.org/10.1021/es405819p.

Caldeira K. and Wickett M. E. (2003) Anthropogenic carbon and ocean pH. *Nature* **425**, 365. https://doi.org/10.1038/425365a.

Carter B. R., Feely R. A., Mecking S., Cross J. N., Macdonald A. M., Siedlecki S. A., Talley L. D., Sabine C. L., Millero F. J., Swift J. H., Dickson A. G. and Rodgers K. B. (2017) Two decades of Pacific anthropogenic carbon storage and ocean acidification along Global Ocean Ship-based Hydrographic Investigations Program sections P16 and P02. *Global Biogeochem. Cycles* **31**, 306–327. https://doi.org/10.1002/2016gb005485.

Carter B. R., Sonnerup R. E., Millero F. J., Woosley R. J., Wanninkhof R., Feely R. A., Hansell D. A., Bullister J. L., Mordy C., Baringer M. O., Langdon C., Key R. M., McNichol A., Doney S. C. and Johnson G. C. (2018) Carbon dioxide, hydrographic and chemical data collected from profile discrete samples during the NOAA Ship Ronald H. Brown cruise RB-16-06 along the GO-SHIP Repeat Hydrography Section P18 (EXPOCODE 33RO20161119) in the Pacific Ocean from 2016–11-19 to 2017–02-03 (NCEI Accession 0171546). NOAA National Centers for Environmental Information, Dataset. https://doi.org/10.7289/v5cv4g1w.

Clayton T. D. and Byrne R. H. (1993) Spectrophotometric seawater pH measurements: total hydrogen ion concentration scale calibration of m-cresol purple and at-sea results. *Deep Sea Res. Part I. Oceanogr. Res. Papers* **40**, 2115–2129. https://doi.org/10.1016/0967-0637(93)90048-8.

Cross J. N., Macdonald A. M., Alin S. R., Wanninkhof R., Dickson A. G., Carlson C. A., Johnson G. C., Baringer M. O., Mordy C., Langdon C., Key R. M., McNichol A., Bullister J. L., Jenkins W. J. and Nelson N. (2017) Dissolved inorganic carbon (DIC), total alkalinity, pH on total scale, dissolved organic carbon (DOC), chlorofluorocarbons (CFC-11, CFC-12), temperature, salinity and other hydrographic and chemical variables collected from discrete samples and profile observations during the R/V Ronald H. Brown cruise along the GO-SHIP Section P16N_2015, Legs 1 and 2 (EXPOCODEs 33RO20150410 and 33RO20150525) in the Pacific Ocean, from 2015–04-10 to 2015–06-27 (NCEI Accession 0163182). NOAA National Centers for Environmental Information, Dataset. https://doi.org/10.3334/cdiac/otg.go_ship_p16n_2015.

Dickson A. G. (1990) Standard potential of the reaction: $AgCl(s) + 12H_2(g) = Ag(s) + HCl(aq)$, and and the standard acidity constant of the ion HSO_4^- in synthetic sea water from 273.15 to 318.15 K. *J. Chem. Thermodyn.* **22**, 113–127. https://doi.org/10.1016/0021-9614(90)90074-Z.

Dickson A. and Millero F. J. (1987) A comparison of the equilibrium constants for the dissociation of carbonic acid in seawater media. *Deep Sea Res. Part A. Oceanogr. Res. Papers* **34**, 1733–1743. https://doi.org/10.1016/0198-0149(87)90021-5.

Dickson A., Sabine C. L., & Christian J. R. (Eds.) (2007) Guide to best practices for ocean CO2 measurements, vol. 3. PICES Special Publication, pp.191.

Doney S. C., Ruckelshaus M., Duffy J. E., Barry J. P., Chan F., English C. A., Galindo H. M., Grebmeier J. M., Hollowed A. B., Knowlton N., Polovina J., Rabalais N. N., Sydeman W. J. and Talley L. D. (2012) Climate change impacts on marine ecosystems. *Annu. Rev. Mar. Sci.* **4**, 11–37. https://doi.org/10.1146/annurev-marine-041911-111611.

Feely R. A., Alin S. R., Hales B., Johnson G. C., Juranek L. W., Byrne R. H., Peterson W. T., Goni M., Liu X. and Greeley D.

(2016) Dissolved inorganic carbon, pH, alkalinity, temperature, salinity and other variables collected from discrete sample and profile observations using Alkalinity titrator, CTD and other instruments from WECOMA in the Gulf of the Farallones National Marine Sanctuary, Monterey Bay National Marine Sanctuary and others from 2011–08-12 to 2011–08-30 (NCEI Accession 0157458). NOAA National Centers for Environmental Information, Dataset. https://accession.nodc.noaa.gov/0157458.

Feely R. A., Sabine C. L., Lee K., Berelson W., Kleypas J., Fabry V. J. and Millero F. J. (2004) Impact of anthropogenic CO_2 on the $CaCO_3$ system in the oceans. *Science* **305**, 362–366. https://doi.org/10.1126/science.1097329.

Fong M. B. and Dickson A. G. (2019) Insights from GO-SHIP hydrography data into the thermodynamic consistency of CO_2 system measurements in seawater. *Mar. Chem.* **211**, 52–63. https://doi.org/10.1016/j.marchem.2019.03.006.

Goyet C. and Poisson A. (1989) New determination of carbonic acid dissociation constants in seawater as a function of temperature and salinity. *Deep Sea Res. Part A. Oceanogr. Res. Papers* **36**, 1635–1654. https://doi.org/10.1016/0198-0149(89)90064-2.

Gruber N., Clement D., Carter B. R., Feely R. A., van Heuven S., Hoppema M., Ishii M., Key R. M., Kozyr A., Lauvset S. K., Lo Monaco C., Mathis J. T., Murata A., Olsen A., Perez F. F., Sabine C. L., Tanhua T. and Wanninkhof R. (2019) The oceanic sink for anthropogenic CO_2 from 1994 to 2007. *Science* **363**, 1193–1199. https://doi.org/10.1126/science.aau5153.

Hansson I. (1973) The determination of the dissociation constants of carbonic acid in synthetic sea water in the salinity range of 20–40‰ and temperature range of 5–30 °C. *Acta Chem. Scand.* **27**, 931–944. https://doi.org/10.3891/acta.chem.scand.27-0931.

Kim H.-C. and Lee K. (2009) Significant contribution of dissolved organic matter to seawater alkalinity. *Geophys. Res. Lett.* **36**. https://doi.org/10.1029/2009GL040271.

Kolthoff I. M. and Stenger V. A. (1964) Volumetric analysis. acid-base, precipitation, and complex-formation reactions, Vol. 2. Interscience, New York.

Le Quéré C., Andrew R. M., Friedlingstein P., Sitch S., Hauck J., Pongratz J., Pickers P. A., Korsbakken J. I., Peters G. P., Canadell J. G., Arneth A., Arora V. K., Barbero L., Bastos A., Bopp L., Chevallier F., Chini L. P., Ciais P., Doney S. C., Gkritzalis T., Goll D. S., Harris I., Haverd V., Hoffman F. M., Hoppema M., Houghton R. A., Hurtt G., Ilyina T., Jain A. K., Johannessen T., Jones C. D., Kato E., Keeling R. F., Goldewijk K. K., Landschützer P., Lefèvre N., Lienert S., Liu Z., Lombardozzi D., Metzl N., Munro D. R., Nabel J. E. M. S., Nakaoka S. I., Neill C., Olsen A., Ono T., Patra P., Peregon A., Peters W., Peylin P., Pfeil B., Pierrot D., Poulter B., Rehder G., Resplandy L., Robertson E., Rocher M., Rödenbeck C., Schuster U., Schwinger J., Séférian R., Skjelvan I., Steinhoff T., Sutton A., Tans P. P., Tian H., Tilbrook B., Tubiello F. N., van der Laan-Luijkx I. T., van der Werf G. R., Viovy N., Walker A. P., Wiltshire A. J., Wright R., Zaehle S. and Zheng B. (2018) Global carbon budget 2018. *Earth Syst. Sci. Data* **10**, 2141–2194. https://doi.org/10.5194/essd-10-2141-2018.

Lee K., Kim T.-W., Byrne R. H., Millero F. J., Feely R. A. and Liu Y.-M. (2010) The universal ratio of boron to chlorinity for the North Pacific and North Atlantic oceans. *Geochim. Cosmochim. Acta* **74**, 1801–1811. https://doi.org/10.1016/j.gca.2009.12.027.

Lee K., Millero F. J., Byrne R. H., Feely R. A. and Wanninkhof R. (2000) The recommended dissociation constants for carbonic acid in seawater. *Geophys. Res. Lett.* **27**, 229–232. https://doi.org/10.1029/1999gl002345.

Lee K., Millero F. J. and Campbell D. M. (1996) The reliability of the thermodynamic constants for the dissociation of carbonic acid in seawater. *Mar. Chem.* **55**, 233–245. https://doi.org/10.1016/S0304-4203(96)00064-3.

Lewis E. and Wallace D. W. R. (1998) Program developed for CO_2 system calculations. In *ORNL/CDIAC-105*. Carbon Dioxide Inf. Anal. Cent., Oak Ridge Natl. Lab., Oak Ridge, Tenn., p. 38, https://salish-sea.pnnl.gov/media/ORNL-CDIAC-105.pdf.

Liu X., Patsavas M. C. and Byrne R. H. (2011) Purification and characterization of meta-cresol purple for spectrophotometric seawater pH measurements. *Environ. Sci. Technol.* **45**, 4862–4868. https://doi.org/10.1021/es200665d.

Lueker T. J., Dickson A. G. and Keeling C. D. (2000) Ocean pCO_2 calculated from dissolved inorganic carbon, alkalinity, and equations for K_1 and K_2: validation based on laboratory measurements of CO_2 in gas and seawater at equilibrium. *Mar. Chem.* **70**, 105–119. https://doi.org/10.1016/S0304-4203(00)00022-0.

Macdonald A. M., Wanninkhof R., Dickson A. G., Carlson C. A., Key R. M., Becker S., Swift J. H., McNichol A., Schlosser P. and Fripiat F. (2018) Discrete profile measurements of dissolved inorganic carbon, total alkalinity, pH and other hydrographic and chemical data obtained during the R/V Roger Revelle Repeat Hydrography and SOCCOM Cruise in the Indian Ocean and Southern Ocean: GO-SHIP Section I08S, (EXPOCODE 33RR20160208) from 2016–02-08 to 2016–03-16 (NCEI Accession 0171457). NOAA National Centers for Environmental Information, Dataset. https://doi.org/10.7289/v5hm56qr.

McLaughlin K., Weisberg S. B., Dickson A. G., Hofmann G. E., Newton J. A., Aseltine-Neilson D., Barton A., Cudd S., Feely R. A., Jefferds I. W., Jewett E. B., King T., Langdon C. J., McAfee S., Pleschner-Steele D. and Steele B. (2015) Core principles of the California current acidification network: Linking chemistry, physics, and ecological effects. *Oceanography* **28**, 160–169.

Mehrbach C., Culberson C., Hawley J. and Pytkowicx R. (1973) Measurement of the apparent dissociation constants of carbonic acid in seawater at atmospheric pressure. *Limnol. Oceanogr.* **18**, 897–907. https://doi.org/10.4319/lo.1973.18.6.0897.

Millero F. J., Graham T. B., Huang F., Bustos-Serrano H. and Pierrot D. (2006) Dissociation constants of carbonic acid in seawater as a function of salinity and temperature. *Mar. Chem.* **100**, 80–94. https://doi.org/10.1016/j.marchem.2005.12.001.

Millero F. J., Pierrot D., Lee K., Wanninkhof R., Feely R., Sabine C. L., Key R. M. and Takahashi T. (2002) Dissociation constants for carbonic acid determined from field measurements. *Deep Sea Res. Part I. Oceanogr. Res. Papers* **49**, 1705–1723. https://doi.org/10.1016/S0967-0637(02)00093-6.

Mojica Prieto F. J. and Millero F. J. (2002) The values of $pK_1 + pK_2$ for the dissociation of carbonic acid in seawater. *Geochim. Cosmochim. Acta* **66**, 2529–2540. https://doi.org/10.1016/S0016-7037(02)00855-4.

Müller J. D. and Rehder G. (2018) Metrology of pH measurements in brackish waters—part 2: experimental characterization of purified meta-Cresol Purple for spectrophotometric pH_T measurements. *Front. Mar. Sci.* **5**, 1–9. https://doi.org/10.3389/fmars.2018.00177.

Naviaux J. D., Subhas A. V., Dong S., Rollins N. E., Liu X., Byrne R. H., Berelson W. M. and Adkins J. F. (2019) Calcite dissolution rates in seawater: Lab vs. in-situ measurements and inhibition by organic matter. *Mar. Chem.* **215**. https://doi.org/10.1016/j.marchem.2019.103684 103684.

Orr J. C., Epitalon J.-M., Dickson A. G. and Gattuso J.-P. (2018) Routine uncertainty propagation for the marine carbon dioxide system. *Mar. Chem.* **207**, 84–107. https://doi.org/10.1016/j.marchem.2018.10.006.

Papadimitriou S., Loucaides S., Rérolle V. M. C., Kennedy P., Achterberg E. P., Dickson A. G., Mowlem M. and Kennedy H. (2018) The stoichiometric dissociation constants of carbonic acid in seawater brines from 298 to 267 K. *Geochim. Cosmochim. Acta* **220**, 55–70. https://doi.org/10.1016/j.gca.2017.09.037.

Patsavas M. C., Byrne R. H., Wanninkhof R., Feely R. A. and Cai W.-J. (2015) Internal consistency of marine carbonate system measurements and assessments of aragonite saturation state: Insights from two US coastal cruises. *Mar. Chem.* **176**, 9–20. https://doi.org/10.1016/j.marchem.2015.06.022.

Riebesell U., Zondervan I., Rost B., Tortell P. D., Zeebe R. E. and Morel F. M. (2000) Reduced calcification of marine plankton in response to increased atmospheric CO_2. *Nature* **407**, 364–367. https://doi.org/10.1038/35030078.

Roy R. N., Roy L. N., Vogel K. M., Porter-Moore C., Pearson T., Good C. E., Millero F. J. and Campbell D. M. (1993) The dissociation constants of carbonic acid in seawater at salinities 5 to 45 and temperatures 0 to 45 °C. *Mar. Chem.* **44**, 249–267. https://doi.org/10.1016/0304-4203(93)90207-5.

Sharp J. D. and Byrne R. H. (2020) Interpreting measurements of total alkalinity in marine and estuarine waters in the presence of proton-binding organic matter. *Deep Sea Res. Part I. Oceanogr. Res. Papers* **103338**. https://doi.org/10.1016/j.dsr.2020.103338.

Sharp, J. D., Pierrot, D., Humphreys, M. P., Epitalon, J.-M., Orr, J. C., Lewis, E. R., & Wallace, D. W.R. (2020). CO2SYSv3 for MATLAB (Version v3.0.1). Zenodo. http://doi.org/10.5281/zenodo.3952803.

Sulpis O., Lauvset S. K. and Hagens M. (2020) Current estimates of K_1* and K_2* appear inconsistent with measured CO_2 system parameters in cold oceanic regions. *Ocean Sci.* **16**, 847–862. https://doi.org/10.5194/os-16-847-2020.

Swift J. H., Mecking S., Feely R. A., Dickson A. G., Carlson C. A., Jenkins W. J., McNichol A., Key R. M., Ho D. T., Sigman D., Macdonald A. M., Buesseler K. and Martz T. R. (2014) Dissolved inorganic carbon, pH, alkalinity, temperature, salinity and other variables collected from discrete sample and profile observations using CTD, bottle and other instruments from MELVILLE in the North Pacific Ocean and Philippine Sea from 2013–03-21 to 2013–05-01 (NCEI Accession 0117338). NOAA National Centers for Environmental Information, Dataset. https://doi.org/10.3334/cdiac/otg.goship_p02_318m20130321.

Talley L. D., Feely R. A., Dickson A. G., Swift J. H., Carlson C. A., Warner M. J., McNichol A., Key R. M. and Schlosser P. (2016) Dissolved inorganic carbon (DIC), total alkalinity, pH on total scale, dissolved organic carbon (DOC), chlorofluorocarbons, temperature, salinity and other hydrographic and chemical variables collected from discrete samples and profile observations during the R/V Nathaniel B. Palmer cruise GOSHIP_P16S_2014 (EXPOCODE 320620140320) in the South Pacific Ocean from 2014–03-20 to 2014–05-05 (NCEI Accession 0157621). NOAA National Centers for Environmental Information, Dataset. https://doi.org/10.3334/cdiac/otg.go_ship_p16s_2014.

Uppström L. R. (1974) The boron/chlorinity ratio of deep-sea water from the Pacific Ocean. *Deep Sea Res. Oceanogr. Abstr.* **21**, 161–162. https://doi.org/10.1016/0011-7471(74)90074-6.

van Heuven S., Pierrot D., Rae J., Lewis E. and Wallace D. (2011) MATLAB program developed for CO2 system calculations. *ORNL/CDIAC-105b. Carbon Dioxide Inf. Anal. Cent., Oak Ridge Natl. Lab., US Dept. of Energy, Oak Ridge, Tenn.*.

Wanninkhof R., Feely R. A., Dickson A. G., Hansell D. A., Key R. M., Swift J. H., Smethie, Jr., W. M., Fine R. A., Jenkins W. J., McNichol A., McCartney M. S. and Druffel E. R. M. (2013) *Partial pressure (or fugacity) of carbon dioxide, dissolved inorganic carbon, pH, alkalinity, temperature, salinity and other variables collected from discrete sample and profile observations using Alkalinity titrator, CTD and other instruments from ATLANTIS in the North Atlantic Ocean from 2012–04-19 to 2012–05-15 (NCEI Accession 0108160)*. NOAA National Centers for Environmental Information, Dataset. https://doi.org/10.3334/cdiac/otg.clivar_a20_2012.

Wanninkhof R., Lewis E., Feely R. A. and Millero F. J. (1999) The optimal carbonate dissociation constants for determining surface water pCO_2 from alkalinity and total inorganic carbon. *Mar. Chem.* **65**, 291–301. https://doi.org/10.1016/S0304-4203(99)00021-3.

Wanninkhof R., Zhang J.-Z., Baringer M. O., Langdon C., Cai W.-J., Salisbury J. E. and Byrne R. H. (2016) *Partial pressure (or fugacity) of carbon dioxide, dissolved inorganic carbon, pH, alkalinity, temperature, salinity and other variables collected from discrete sample and profile observations using CTD, bottle and other instruments from NOAA Ship RONALD H. BROWN in the Gray's Reef National Marine Sanctuary, Gulf of Mexico and North Atlantic Ocean from 2012-07-21 to 2012-08-13 (NCEI Accession 0157619)*. NOAA National Centers for Environmental Information, Dataset. https://doi.org/10.3334/cdiac/otg.coastal_gomecc2.

Waters J. F. and Millero F. J. (2013) The free proton concentration scale for seawater pH. *Mar. Chem.* **149**, 8–22. https://doi.org/10.1016/j.marchem.2012.11.003.

Waters J., Millero F. J. and Woosley R. J. (2014) Corrigendum to "The free proton concentration scale for seawater pH", [MARCHE: 149 (2013) 8–22]. *Mar. Chem.* **165**, 66–67. https://doi.org/10.1016/j.marchem.2012.11.003.

Wittmann A. C. and Pörtner H.-O. (2013) Sensitivities of extant animal taxa to ocean acidification. *Nat. Clim. Change* **3**, 995–1001. https://doi.org/10.1038/nclimate1982.

Woosley R. J. (2018) Complexity of marine CO_2 system highlighted by seasonal asymmetries. *Global Biogeochem. Cycles* **32**, 1434–1436. https://doi.org/10.1029/2018GB006081.

Yao W. and Byrne R. H. (2001) Spectrophotometric determination of freshwater pH using bromocresol purple and phenol red. *Environ. Sci. Technol.* **35**, 1197–1201.

Associate editor: Alfonso Mucci